

Chemoinformatic Approaches in the Study of Fluralaner and Afoxolaner-mediated Inhibition of l-glutamate-gated Chloride Channels

Douglas Vieira Thomaz¹, Edson Silvio Batista Rodrigues¹, Isaac Yves Lopes de Macedo¹

¹ Universidade Federal de Goiás

240 street, Leste Universitário district, Goiânia - GO, 74605-170, Brazil

DOI: [10.22178/pos.44-6](https://doi.org/10.22178/pos.44-6)

LCC Subject Category: [RM1-950](#)

Received 27.02.2019


Accepted 27.03.2019

Published online 31.03.2019

Corresponding Author:

Douglas Vieira Thomaz

douglasvthomaz@gmail.com

© 2019 The Authors. This article is licensed under a [Creative Commons Attribution 4.0 License](#) 

Abstract. This work showcased the chemoinformatic study of isoxazoline ectoparasiticides: Fluralaner (FLU) and Afoxolaner (AFO) interactions with l-glutamate-gated chloride channels (3RHW). In order to evaluate inhibition thermodynamics, computational approaches such as molecular docking were employed. Results evidenced that FLU-3RHW highest scoring pose presented lower Gibbs free energy and henceforth, lower K_i values than AFO-3RHW. The findings herein reported suggest therefore that computational methods might be useful to study the thermodynamic features of ectoparasiticides used in veterinary care, what might shed further light on their chemical and pharmacological properties.

Keywords: ectoparasite; molecular docking; ion channel; HOMO; pharmacodynamics.

INTRODUCTION

Fluralaner (FLU) and Afoxolaner (AFO) are widely prescribed isoxazoline ectoparasiticides in veterinary care against flea and tick infestations. Owing to their lipophilic chemical structures, their presence in animal tissue can be extended up to twelve weeks according to dose and patient weight. These compounds exert their pharmacological activities through the inhibition of γ -aminobutyric acid (GABA)-gated chloride channels and l-glutamate-gated chloride channels which are present in ectoparasite cells [1, 2, 3, 4].

FLU and AFO have remarkable efficacy as antiparasitic agents whose are nonetheless also associated with noteworthy safety, hence toxicity cases have been rarely reported. These compounds are known to inhibit chlorine channels similarly to other antiparasitary compounds such as ivermectin. Amongst these channels, l-glutamate-gated are remarkable due to their involvement in ectoparasite vital functions [5, 6, 7, 8].

Although literature supports the pharmacological properties of these compounds, there was, to the best of our knowledge, no report regarding

an *in silico* investigation of their inhibition thermodynamic towards their therapeutic targets. In this context, molecular docking strategies might provide important insights concerning the pharmacodynamics of isoxazoline ectoparasiticides. As showcased by previous reports by our group and literature, *in silico* tools can be applied to comprehensively assess overall physicochemical features which might foment insights about the mechanism of action of drugs [9, 10, 11].

In view of the importance of better understanding FLU and AFO mechanisms of action in veterinary care, this work is aimed on the *in silico* study of the thermodynamics of the inhibition promoted by these drugs on l-glutamate-gated chloride channels.

METHODS

In silico methods. The protocol herein depicted is based on previous reports by our group [10, 11] in which ligands were studied concerning their kinetic and thermodynamic parameters regarding macromolecule i.e. protein/channel inhibition: FLU (4-[5-(3,5-dichlorophenyl)-5-(trifluoromethyl)-4H-1,2-oxazol-3-yl]-2-methyl-N-[2-oxo-2-(2,2,2-trifluoroethylamino)ethyl]benzamide)

and AFO (4-[5-[3-chloro-5-(trifluoromethyl)phenyl]-5-(trifluoromethyl)-4H-1,2-oxazol-3-yl]-N-[2-oxo-2-(2,2,2-trifluoroethylamino)ethyl]naphthalene-1-carboxamide) structures were minimized through Chimera software version 1.13 coupled to *Molecular Modeling Toolkit* (MMTK) and *AMBER toolkit* 4.0 prior docking studies. The same software was used to edit protein units retrieved from *Protein DataBank* (PDB).

Moreover, the software *Python Molecular Viewer* (PMV) version 1.5.6 was used to evaluate torsion-prone regions in each analyzed molecule, namely: FLY and AFO, and the docking models were conducted using *AutoDock Vina* and *AutoDock Tools* version 1.5.6. The docking models herein employed are based on a flexible ligand and a rigid receptor, therefore configuring itself as a semi-flexible model [12, 13, 14]. The minimization in energy conformation and HOMO surface calculations were performed employing MM2 Force Field in ChemDraw3D® Pro 12.

l-glutamate-gated chloride channel structure (3RHW). In this work was employed *C. elegans* glutamate-gated chloride channel receptor (PDB entry: 3RHW) in complex with ivermectin. The chemical structure of the original ligand *i.e.* ivermectin was deleted and the ligand site was used in the docking-grid to guide inhibition analysis. The docking-grid was adjusted to encompass all possible interaction sites where ivermectin was previously bound. Exhaustiveness was set to 20 in order to render more reproducible results.

Inhibition constants calculation. The values of Gibbs free energy are associated to the energy level of thermodynamic systems, and might be correlated to the feasibility of stable intermolecular interactions. Therefore, this parameter was analyzed and used to calculate the inhibition constant (K_i) through the following equation (1):

$$\Delta G = RT \ln K_i, \quad (1)$$

where ΔG is the Gibbs free energy of the system; R is the gas constant and T is the temperature.

This equation can be derived as shown bellow (2).

$$K_i = \frac{\Delta G}{e^{RT}}, \quad (2)$$

where e is the Euler number.

All theoretical applications herein depicted were previously showcased in previous reports by our group [10, 11].

RESULTS AND DISCUSSION

FLU and AFO energy minimization. In order to prepare each molecule for docking, their energies were minimized to render the lowest energy conformer. Moreover, highest occupied molecular orbital (HOMO) regions were also calculated as well as the torsion-feasible regions. Results are displayed in Figure 1.

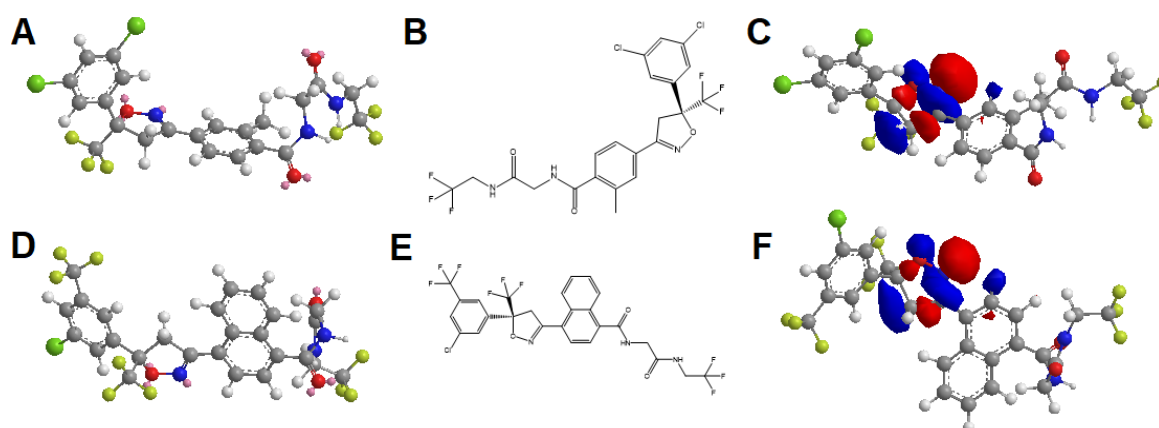


Figure – Results of FLU and AFO energy minimization

Notes: A) 3D Chemical structure of FLU lowest energy conformer; B) 2D chemical depiction of FLU structure; C) HOMO depictions of CBP lowest energy conformer depicting low (Blue) and high (Red) electron density regions; D) 3D Chemical structure of AFO lowest energy conformer; E) 2D chemical depiction of AFO structure; F) HOMO depictions of AFO lowest energy conformer depicting low (Blue) and high (Red) electron density regions. All data gathered through Chimera software version 1.13.

Results evidenced that in both FLU and AFO lowest energy conformers, the oxazolic moiety presents a bend shape (Figure 1). Furthermore, HOMO regions of the molecules showcased that the oxazolic moiety is also the main group which could be covalently bonded to a macromolecule in a possible coupling mechanism involving electron sharing (Figure 1). Concerning torsion-prone regions, both in FLU and AFO, the terminal aliphatic chain, which present $\sigma^{sp^3-sp^3}$ covalent bounds, is the main flexible moiety.

FLU and AFO docking to 3RHW. In order to explore FLU inhibition of 3RHW, a molecular docking approach was used. Henceforth the gridline for the docking study was set around the region originally occupied by ivermectin in the crystallographic data retrieved from PDB. Figure 2 displays the highest scoring model with the distances between FLU and nearby residues measured in angstroms (Å).

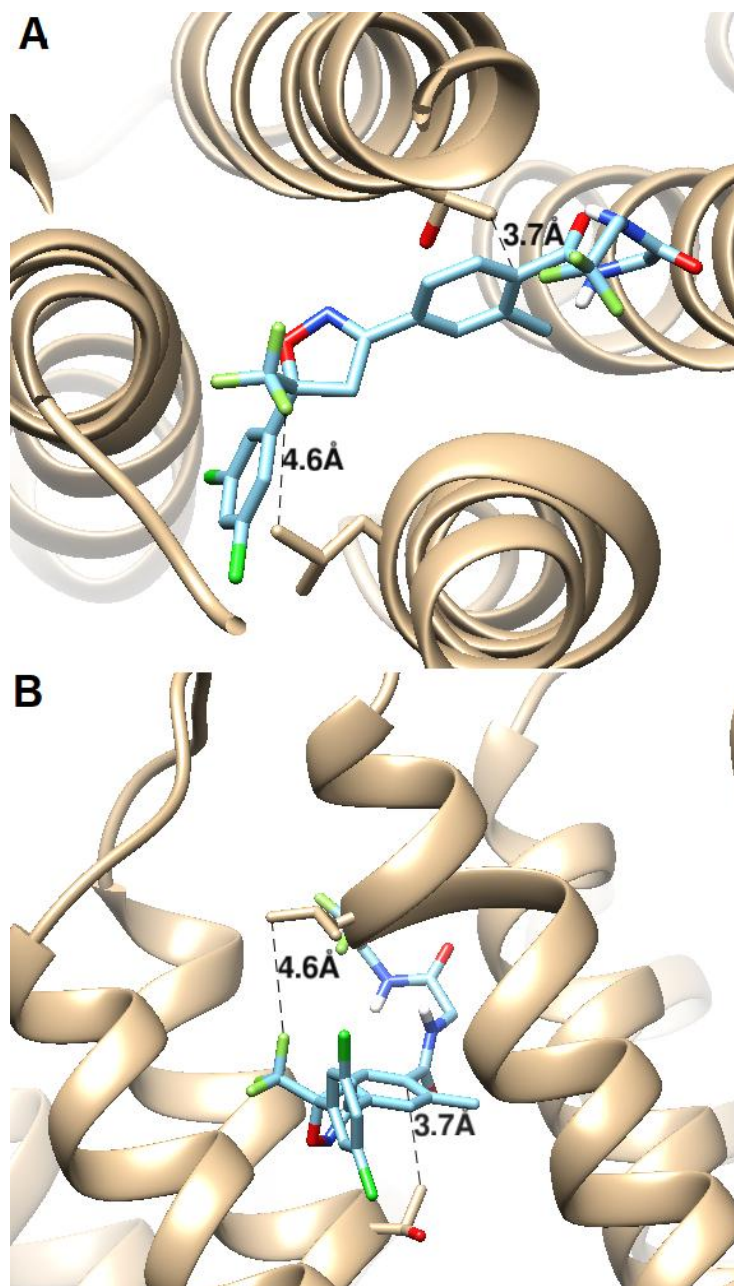


Figure 2– FLU and AFO docking to 3RHW

Notes: Molecular docking depiction of the highest scoring model for FLU-3RHW interaction. Distances therein highlighted between FLU molecule (Blue, Red and Green) and nearby residues measured in angstroms (Å). All data gathered through Chimera software version 1.13.

FLU-3RHW highest scoring docking model showcased no hydrogen bonds (Figure 2). The close proximity of the ligand structure to the α -helices of 3RHW, and the low Gibbs free energy associated to this conformation suggests that FLU molecule might stably interact with the macro-molecule in the position therein depicted.

Moreover, the same protocol was used to study AFO-3RHW interaction. Results are depicted in Figure 3, wherein the highest scoring model is showcased.

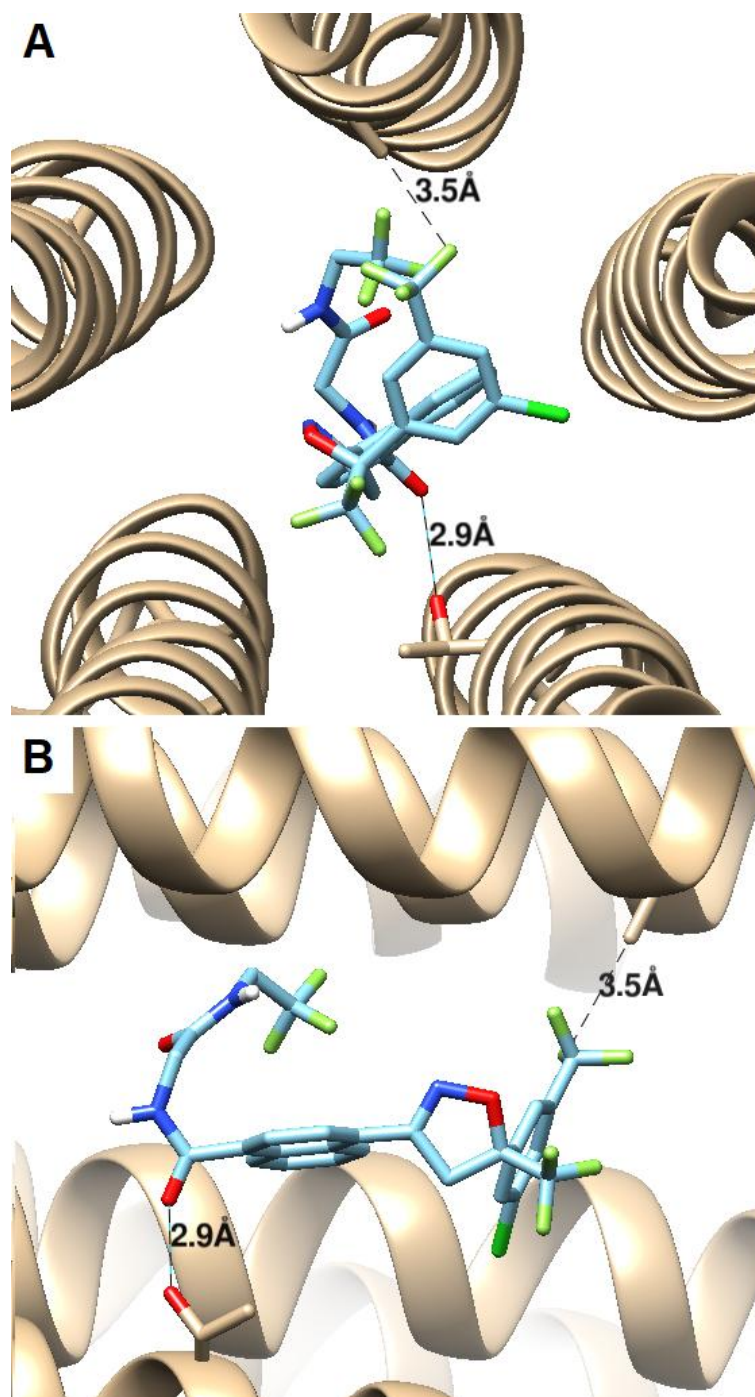


Figure 3 – Results of study AFO-3RHW interaction

Notes: Molecular docking depiction of the highest scoring model for AFO-3RHW interaction. Distances therein highlighted between AFO molecule (Blue, Red and Green) and nearby residues measured in angstroms (Å). All data gathered through Chimera software version 1.13

AFO-3RHW highest scoring model was located between the α -helices of the pentameric-structured moiety of the macromolecule. Furthermore, the model presented a hydrogen bond (Figure 3).

Considering that the docking-grids were assigned to encompass all possible inhibition sites in 3RHW molecule, which were originally occupied by ivermectin, the presence of FLU and AFO in these pockets suggests interaction and might be correlated to the biological activities of these drugs [15, 16, 17, 18]. Nonetheless, FLU and AFO inhibition of l-glutamate-gated chloride channels is well reported in literature, what corroborates to the results herein showcased [1, 2, 3, 4].

Furthermore, the low energy values associated to each pose further suggests interaction, hence

small energy models are usually associated to higher stability, and therefore feasible interaction [19, 20, 21, 22]. Nonetheless, literature reports corroborate to these findings in both models [23, 24].

In order to gather more information about the thermodynamic features of the calculated docking models and establish correlations to their pharmacological applications, their K_i were calculated from the Gibbs free energy of each highest scoring pose.

Inhibition constant calculation. The K_i of the lowest energy pose for both FLU-3RHW and AFO-3RHW was calculated and displayed below in Table 1.

Table 1 – Thermodynamical properties calculated for the lowest energy pose of FLU-3RHW and AFO-3RHW

| Model | Affinity, kcal.mol ⁻¹ | K_i , cal.mol ⁻¹ K ⁻¹ 10 ⁻⁸ | RMSD, l. b. | RMSB, u. b. | HBonds, ligand | HBonds, receptor |
|----------|----------------------------------|--|-------------|-------------|----------------|------------------|
| FLU-3RHW | -9.8 | 7.247 | 0.0 | 0.0 | 0 | 0 |
| AFO-3RHW | -8.9 | 32.808 | 0.0 | 0.0 | 1 | 1 |

Results evidenced that the calculated K_i for FLU-3RHW was lower than that of AFO-3RHW, what suggest higher thermodynamic feasibility of the inhibition promoted by FLU molecule. This is a remarkable finding, since no previous work has reported the difference between FLU and AFO interactions with their biological targets through computational methods. Albeit the results of this work suggest that FLU may interact more to l-glutamate-gated chloride channels than AFO could, more investigations are needed to better understand the pharmacodynamics of these isoxazoline ectoparasiticides.

CONCLUSION

This work showcased the *in silico* study of FLU and AFO interactions with l-glutamate-gated chloride channels, wherein FLU-3RHW highest scoring pose presented lower Gibbs free energy and henceforth, lower K_i values than AFO-3RHW. The findings herein reported suggest therefore that computational methods might be useful to study the thermodynamic features of isoxazoline ectoparasiticides, what might shed further light on their chemical and pharmacological properties.

REFERENCES

- Gassel, M., Wolf, C., Noack, S., Williams, H., & Ilg, T. (2014). The novel isoxazoline ectoparasiticide fluralaner: Selective inhibition of arthropod γ -aminobutyric acid- and l-glutamate-gated chloride channels and insecticidal/acaricidal activity. *Insect Biochemistry and Molecular Biology*, 45, 111–124. doi: 10.1016/j.ibmb.2013.11.009
- Liu, D., Jia, Z.-Q., Peng, Y.-C., Sheng, C.-W., Tang, T., Xu, L., ... Zhao, C.-Q. (2018). Toxicity and sublethal effects of fluralaner on *Spodoptera litura* Fabricius (Lepidoptera: Noctuidae). *Pesticide Biochemistry and Physiology*, 152, 8–16. doi: 10.1016/j.pestbp.2018.08.004

3. Sheng, C.-W., Jia, Z.-Q., Liu, D., Wu, H.-Z., Luo, X.-M., Song, P.-P., ... Zhao, C.-Q. (2017). Insecticidal spectrum of fluralaner to agricultural and sanitary pests. *Journal of Asia-Pacific Entomology*, 20(4), 1213–1218. doi: [10.1016/j.aspen.2017.08.021](https://doi.org/10.1016/j.aspen.2017.08.021)
4. Pérez-Sánchez, R., & Oleaga, A. (2017). Acaricidal activity of fluralaner against *Ornithodoros moubata* and *Ornithodoros erraticus* argasid ticks evaluated through in vitro feeding. *Veterinary Parasitology*, 243, 119–124. doi: [10.1016/j.vetpar.2017.06.021](https://doi.org/10.1016/j.vetpar.2017.06.021)
5. Beugnet, F., Liebenberg, J., & Halos, L. (2015). Comparative efficacy of two oral treatments for dogs containing either afoxolaner or fluralaner against *Rhipicephalus sanguineus sensu lato* and *Dermacentor reticulatus*. *Veterinary Parasitology*, 209(1-2), 142–145. doi: [10.1016/j.vetpar.2015.02.002](https://doi.org/10.1016/j.vetpar.2015.02.002)
6. Beugnet, F., Liebenberg, J., & Halos, L. (2015). Comparative speed of efficacy against *Ctenocephalides felis* of two oral treatments for dogs containing either afoxolaner or fluralaner. *Veterinary Parasitology*, 207(3-4), 297–301. doi: [10.1016/j.vetpar.2014.12.007](https://doi.org/10.1016/j.vetpar.2014.12.007)
7. Huang, Q.-T., Sheng, C.-W., Jiang, J., Tang, T., Jia, Z.-Q., Han, Z.-J., & Zhao, C.-Q. (2019). Interaction of insecticides with heteromeric GABA-gated chloride channels from zebrafish *Danio rerio* (Hamilton). *Journal of Hazardous Materials*, 366, 643–650. doi: [10.1016/j.jhazmat.2018.11.085](https://doi.org/10.1016/j.jhazmat.2018.11.085)
8. Sojka, P. A. (2018). Isoxazolines. *Journal of Exotic Pet Medicine*, 27(2), 118–122. doi: [10.1053/j.jepm.2018.02.038](https://doi.org/10.1053/j.jepm.2018.02.038)
9. Amaro, R. E., Baudry, J., Chodera, J., Demir, Ö., McCammon, J. A., Miao, Y., & Smith, J. C. (2018). Ensemble Docking in Drug Discovery. *Biophysical Journal*, 114(10), 2271–2278. doi: [10.1016/j.bpj.2018.02.038](https://doi.org/10.1016/j.bpj.2018.02.038)
10. Thomaz, D. V., Rodrigues, E. S. B., Machado, F. B., ... Macedo, I. Y. L. (2019). Investigation of Cyclobenzaprine Interactions with P450 Cytochromes CYP1A2 and CYP3A4 through Molecular Docking Tools. *Path of Science*, 5(2), 4001–4006. doi: [10.22178/pos.43-1](https://doi.org/10.22178/pos.43-1)
11. Lima Neto, L. F., Barruffini, A. C. C., Machado, F. B., Macedo, I. Y. L., & Thomaz, D. V. (in press). In silico investigation of possible Caffeine interactions with common Inflammation-related targets. *Journal of Applied Biology & Biotechnology*.
12. Trott, O., & Olson, A. J. (2009). AutoDock Vina: Improving the speed and accuracy of docking with a new scoring function, efficient optimization, and multithreading. *Journal of Computational Chemistry*, 31, 455–461. doi: [10.1002/jcc.21334](https://doi.org/10.1002/jcc.21334)
13. Case, D. A., Cheatham, T. E., Darden, T., Gohlke, H., Luo, R., Merz, K. M., ... Woods, R. J. (2005). The Amber biomolecular simulation programs. *Journal of Computational Chemistry*, 26(16), 1668–1688. doi: [10.1002/jcc.20290](https://doi.org/10.1002/jcc.20290)
14. Salomon-Ferrer, R., Case, D. A., & Walker, R. C. (2012). An overview of the Amber biomolecular simulation package. *Wiley Interdisciplinary Reviews: Computational Molecular Science*, 3(2), 198–210. doi: [10.1002/wcms.1121](https://doi.org/10.1002/wcms.1121)
15. Khorasani, R., & Fleming, P. E. (2016). On calculating HR bond enthalpies using computational data. *Computational and Theoretical Chemistry*, 1096, 89–93. doi: [10.1016/j.comptc.2016.09.033](https://doi.org/10.1016/j.comptc.2016.09.033)
16. Kumar, S. P. (2018). PLHINT: A knowledge-driven computational approach based on the intermolecular H bond interactions at the protein-ligand interface from docking solutions. *Journal of Molecular Graphics and Modelling*, 79, 194–212. doi: [10.1016/j.jmgm.2017.12.002](https://doi.org/10.1016/j.jmgm.2017.12.002)
17. Zhang, Q., Bai, P., Zheng, C., Cheng, Y., Wang, T., & Lu, X. (2018). Design, synthesis, insecticidal activity and molecular docking of doramectin derivatives. *Bioorganic & Medicinal Chemistry*. doi: [10.1016/j.bmc.2018.12.040](https://doi.org/10.1016/j.bmc.2018.12.040)
18. Morris, G. M., & Lim-Wilby, M. (2008). Molecular Docking. *Molecular Modeling of Proteins*, 365–382. doi: [10.1007/978-1-59745-177-2_19](https://doi.org/10.1007/978-1-59745-177-2_19)

19. Cosconati, S., Forli, S., Perryman, A. L., Harris, R., Goodsell, D. S., & Olson, A. J. (2010). Virtual screening with AutoDock: theory and practice. *Expert Opinion on Drug Discovery*, 5(6), 597–607. doi: [10.1517/17460441.2010.484460](https://doi.org/10.1517/17460441.2010.484460)
20. Meng, X.-Y., Zhang, H.-X., Mezei, M., & Cui, M. (2011). Molecular Docking: A Powerful Approach for Structure-Based Drug Discovery. *Current Computer Aided-Drug Design*, 7(2), 146–157. doi: [10.2174/157340911795677602](https://doi.org/10.2174/157340911795677602)
21. Lynagh, T., & Lynch, J. W. (2012). Ivermectin binding sites in human and invertebrate Cys-loop receptors. *Trends in Pharmacological Sciences*, 33(8), 432–441. doi: [10.1016/j.tips.2012.05.002](https://doi.org/10.1016/j.tips.2012.05.002)
22. Fuse, T., Kita, T., Nakata, Y., Ozoe, F., & Ozoe, Y. (2016). Electrophysiological characterization of ivermectin triple actions on *Musca* chloride channels gated by l -glutamic acid and γ -aminobutyric acid. *Insect Biochemistry and Molecular Biology*, 77, 78–86. doi: [10.1016/j.ibmb.2016.08.005](https://doi.org/10.1016/j.ibmb.2016.08.005)
23. Gielen, M., & Corringer, P.-J. (2018). The dual-gate model for pentameric ligand-gated ion channels activation and desensitization. *The Journal of Physiology*, 596(10), 1873–1902. doi: [10.1113/jp275100](https://doi.org/10.1113/jp275100)
24. Burgio, F., Meyer, L., & Armstrong, R. (2016). A comparative laboratory trial evaluating the immediate efficacy of fluralaner, afoxolaner, sarolaner and imidacloprid + permethrin against adult *Rhipicephalus sanguineus* (sensu lato) ticks attached to dogs. *Parasites & Vectors*, 9(1). doi: [10.1186/s13071-016-1900-z](https://doi.org/10.1186/s13071-016-1900-z)